Electronic Supplementary Material (ESI) for RSC Advances.

Supporting Information

Tables:

Table S1. SEM-EDXS and AA data of the studied intercalated composites.

	$K_{0,24}[Cu_2(L)]_{0,08}Mn_{0,8}PS_3$.		$K_{0,32}[Zn_2(L)]_{0,04}Mn_{0,8}PS_3$.	
Element	Calc.	Exp.	Calc.	Exp.
% P	16,69	16,3	16,63	15,4
% Mn	23,68	24,4	23,60	24,6
% K	5,06	5,0	6,72	6,9
% S	51,83	50,4	51,65	50,5
% M (Cu^{II}/Zn^{II})	2,74	2,8	1,40	1,3

Figures:

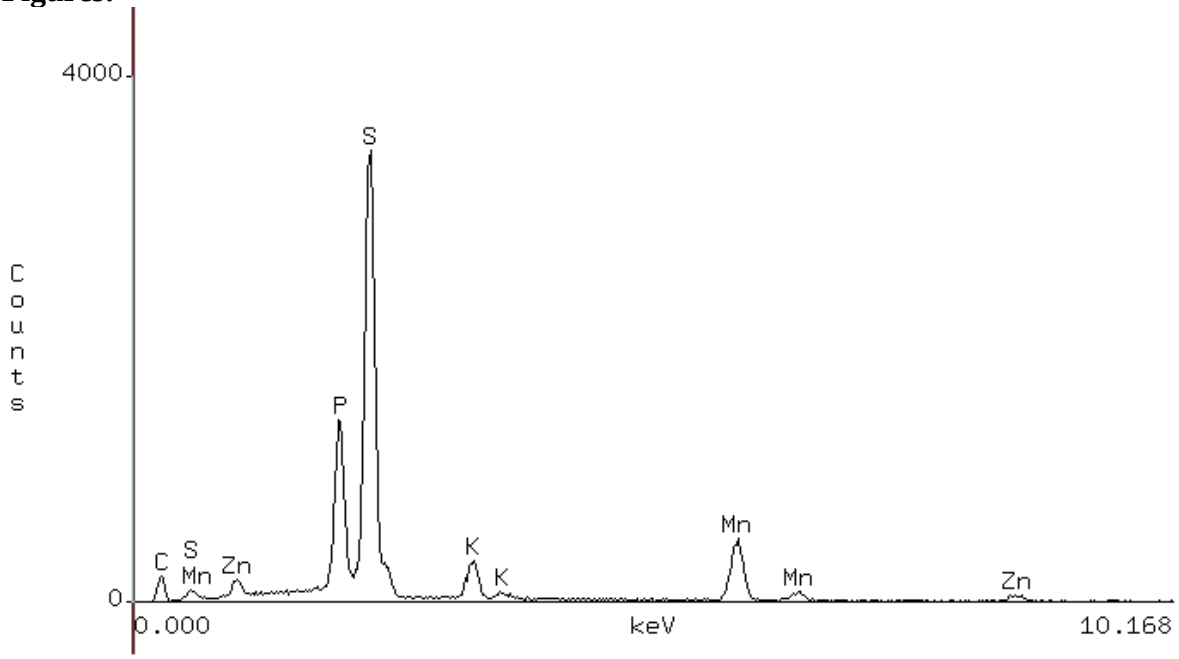

Fig S1. SEM-EDXS spectrum of $K_{0,32}[Zn_2(L)]_{0,04}Mn_{0,8}PS_3$.

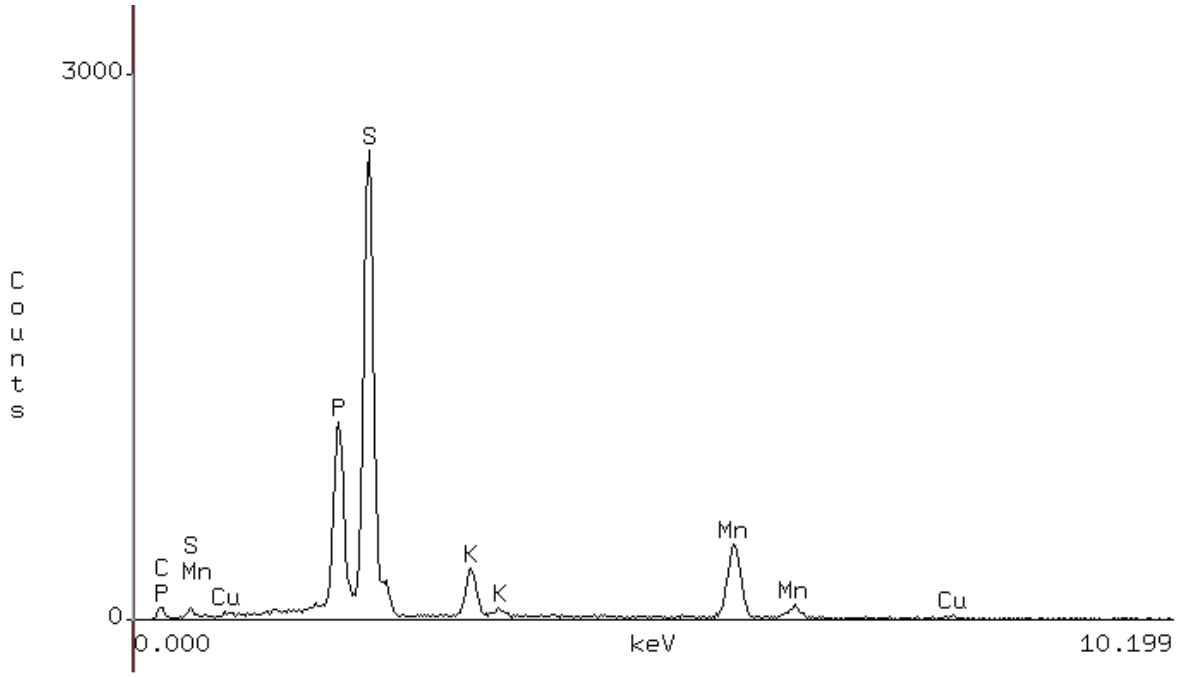

Fig S2. SEM-EDXS spectrum of $K_{0,24}[Cu_2(L)]_{0,08}Mn_{0,8}PS_3$.

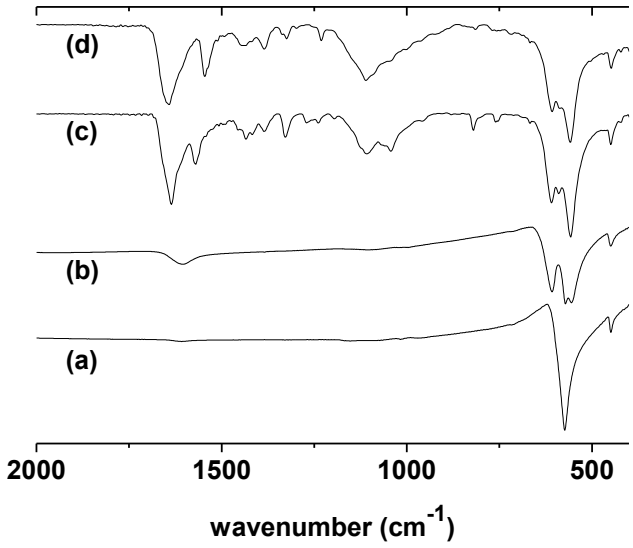

Fig. S3. FTIR of studied phases; (a) pristine $MnPS_3$ phase, (b) potassium precursor $K_{0.4}Mn_{0.8}PS_3 \cdot H_2O$ and composites derived from the intercalation of (c) Zn^{II} complex **(1)** and (d) Cu^{II} complex **(2)**.

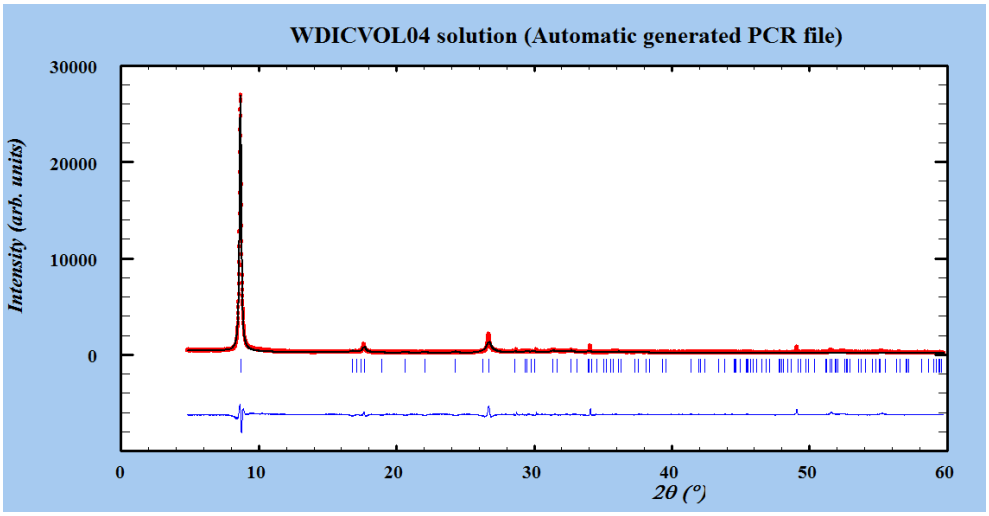

Fig. S4. Simulated X-ray diffractogram of **(1)**

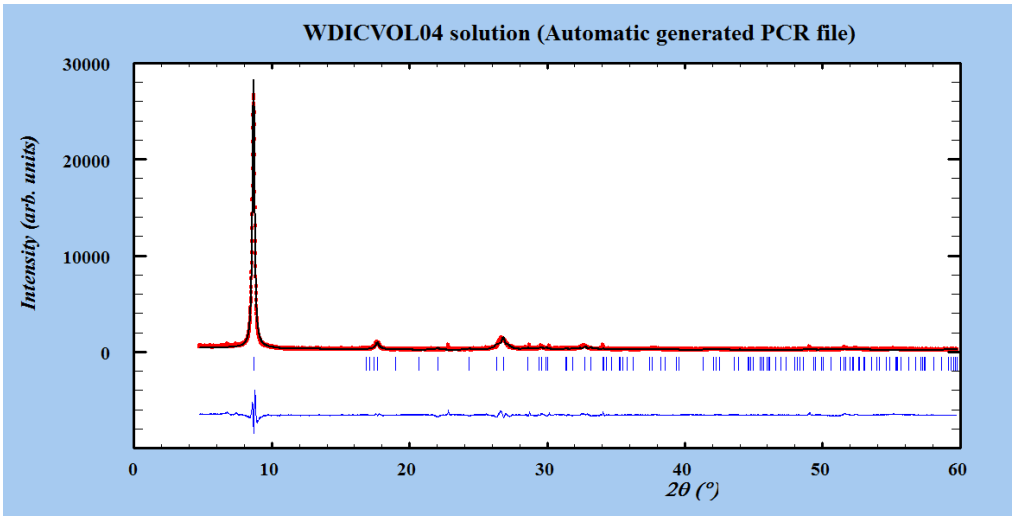

Fig. S5. Simulated X-ray diffractogram of **(2).**

$MnPS_3$

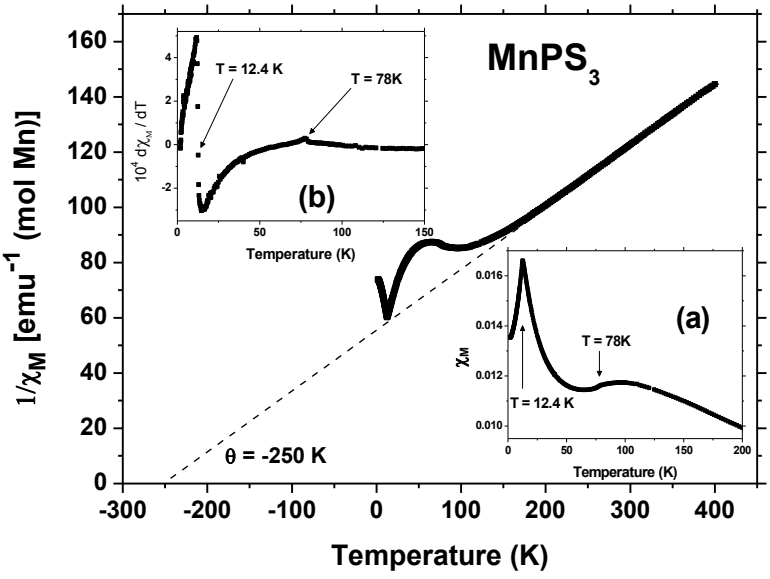

Fig. S6. Plot of the inverse of $\chi_M(T)$ for the pristine phase $MnPS_3$. The dashed line extrapolates the Weiss constant. The insets show (a) the susceptibility and (b) the first derivative, $d\chi_M/dT(T)$, indicating the transition temperatures as explained in the text.

Fig. S6 shows the *dc* susceptibility data of the pristine phase $MnPS_3$. plotted as a function of temperature. Above 200 K the susceptibility curve shows a Curie-Weiss behavior. The molar Curie constant *C* (expressed for a mole of substance) can be extracted from the high temperature $1/\chi_M$ vs. *T* plot of Fig. S6, and results $C = 4.51$ emu K mol^{-1}, allowing to calculate the effective magnetic moment (in units of Bohr magnetons),

$$\mu_{eff} = \sqrt{\frac{3K_B C}{N_A \mu_B^2}} \approx 2.828\sqrt{C} \approx 6.0, \qquad \text{(S1)}$$

where k_B is the Boltzmann constant, N_A is the Avogadro constant, and μ_B the Bohr magneton. The effective magnetic moment calculated by Eq. 1, $\mu_{eff} \approx 6.0$, is slightly above the value expected for a high spin d-system, that one can get from the "spin-only formula", $\mu_{eff} = \sqrt{n(n+2)} = \sqrt{35} \approx 5.92$, where $n = 5$ is the number of unpaired electrons for the Mn^{II}

ion [1]. The plot also gives an estimative of the Weiss constant, $\theta \approx -250\,\mathrm{K}$, indicating antiferromagnetic interactions.

When the temperature decreases below 200 K a broad maximum is observed in the χ_M(T) plot, as shown in the inset (a) in Fig.S6. For a two-dimensional antiferromagnet, the Neel temperature is defined as the temperature at which the slope of the susceptibility vs. temperature curve is a maximum. As can be seen in the inset (b) of Fig. S6, the first derivative of this broad maximum peaks around 78 K, as expected from the literature data. Additionally, a second and sharp peak in the χ_M(T) plot is observed at 12.4 K, that can result from antiferromagnetic coupling between layers, as mentioned in the main text.

In order to further study of the magnetic behavior of the obtained composites, *ac* measurements of the composites at variable temperature and frequencies of 10 and 1000 Hz were carried out. Fig. S7 shows the *ac* susceptibility plots measured for the pristine phase. The imaginary component, χ'', shows no apparent variations, staying close to zero in the entire temperature range for both frequencies, indicating the absence of dissipative processes. The real component, χ', presents a monotonic increase as the temperature decreases from 50 K to about 2 K. In the limit of low frequencies the *ac* measurement is expected to be similar the *dc* measurement, with the real component reproducing the slope of the *M*(*H*) curve, being sensitive to thermodynamic phase changes. However, in the data shown in Fig. S7 neither divergences nor maxima are observed, despite the evidence of a phase transition been detected at 12.4 K in the *dc* susceptibility data of Fig. S6.

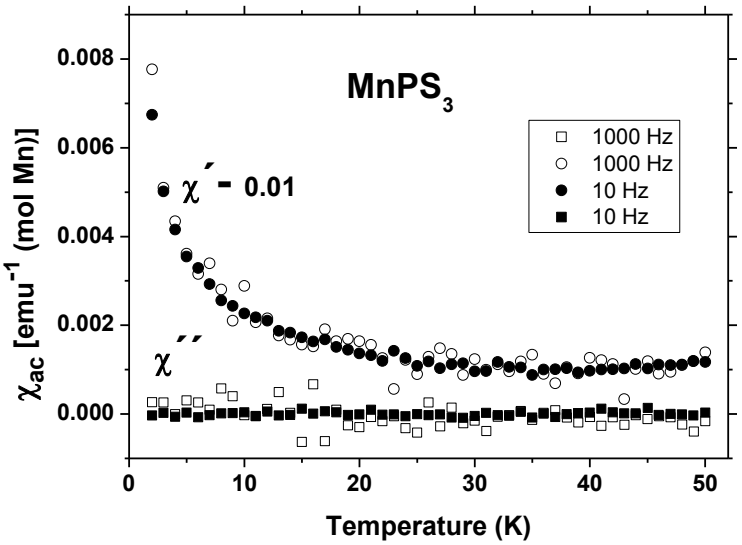

Fig. S7: *ac* susceptibility of $MnPS_3$ as a function of temperature, with a 4 G drive field amplitude. For better clarity, the in-phase component (χ') is shifted down by 0.01 units.

$K_{0.4}Mn_{0.8}PS_3$

Above 60 K the susceptibility curve shows a Curie-Weiss behavior. The molar Curie constant C (expressed for a mole of substance) can be extracted from the high temperature $1/\chi_M$ vs. T plot of Fig. S8 and results C = 3.72 emu K mol^{-1}, giving an effective magnetic moment of 5.45 μ_B.

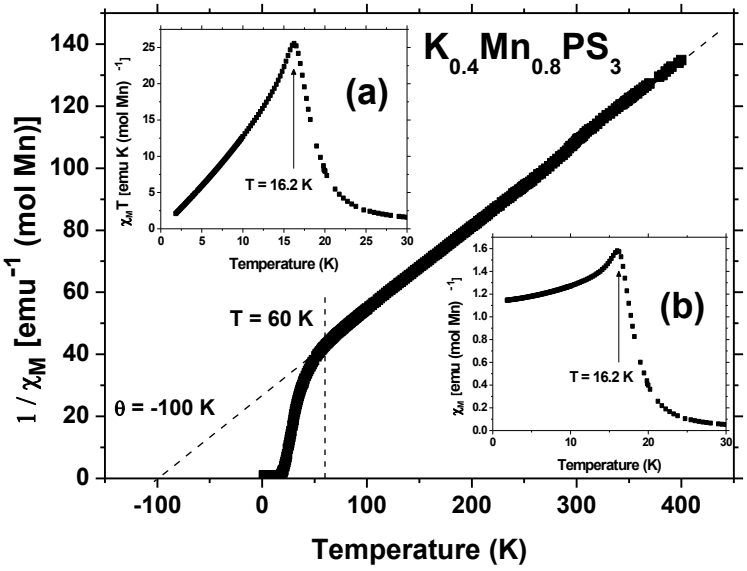

Fig. S8. Plot of the inverse of $\chi_M(T)$ for $K_{0.4}Mn_{0.8}PS_3$ phase. The dashed lines extrapolate the Weiss constant and transition temperature. The insets show (a) the product of the susceptibility by temperature, $\chi_M T(T)$, and (b) the susceptibility $\chi_M(T)$.

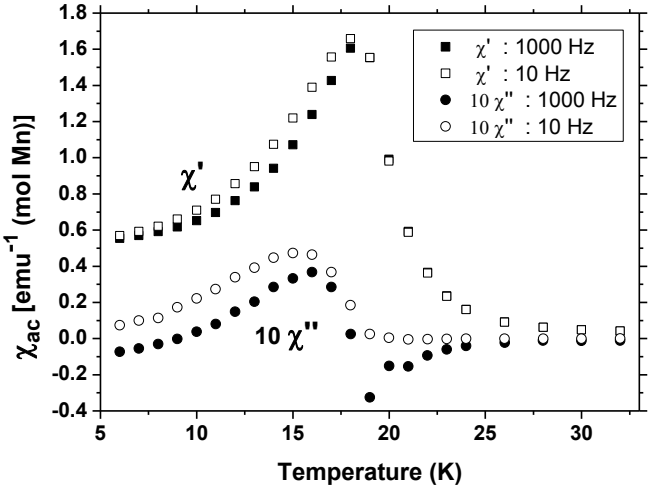

Fig. S9: *ac* Susceptibility of $K_{0.4}Mn_{0.8}PS_3$ phase as a function of temperature, with a 4 G drive field amplitude and frequency of 10 Hz and 1000 Hz. For better clarity, the out-of-phase component (χ'') has been amplified by a factor 10.

References.

(1) R. Lx. Carlin, *Magnetochemistry*, Springer-Verlag, Berlin, 1974, p. 53